

and the reduced normal-state Hall-angle tangent<sup>27</sup>

$$P_n \equiv [\tan\theta_n(H)] / [\tan\theta_n(H_{k20})]. \quad (7)$$

The data are normalized at  $H_{k20}$  [defined by Eq. (1)] rather than  $H_{c20}$  in order to allow a more legitimate comparison of our data with the results of previous experiment<sup>1-8</sup> and theory<sup>9-13</sup> which apply to the low- $H$  domain where electron-spin interaction with  $H$  is presumably unimportant and  $H_{k20} = H_{c20}$ . Strictly speaking, the  $P_m$  data of Fig. 2 represent lower limits<sup>1,4,7</sup> and show that at low  $H/H_{k20}$  the Hall-angle tangent is much larger in the mixed state than in the normal state, i.e.,  $P_m \gg P_n$ , in agreement with the results of the Philips workers<sup>2-4</sup> on low- $\kappa_G$  Nb-Ta alloys. Actually, in view of the discussion centering on Eqs. (3) and (4), we believe that our result

$$P_m(H/H_{k20}=0.35) \approx 0.6, \quad (8)$$

<sup>27</sup> The normal-state Hall data agree with Ref. 18. The normal-state  $\tan\theta_n(H)$  of Fig. 2 is derived from  $J$ -independent  $\tan\theta_n(J)$  and  $\tan\theta_n(H)$  data taken at  $16 < H < 39$  kG and  $T = 4.2^\circ\text{K}$ , where both the mixed state and the sheath (Ref. 15) are suppressed, assuming that the observed direct proportionality of  $\tan\theta_n$  to  $H$  holds for  $0 < H < H_{c20}^*$  and that  $\tan\theta_n$  is  $T$ -independent below  $4.2^\circ\text{K}$ .

obtained at the highest  $H = 39$  kG, is reasonably close to the free-flux-flow  $P_m$  of theoretical interest. Assuming this to be the case and that other Hall measurements reflect the free-flux-flow condition, there appears to be no quantitative agreement of our results with previous experimental or theoretical work:  $P_m(0.35) \approx 2$  (low- $\kappa_G$  Nb-Ta),<sup>4,28</sup> 0.35 (pure Nb),<sup>1,5,8</sup> 1 (pure Nb),<sup>6</sup> 0.35 (Bardeen-Stephen theory),<sup>9</sup> 1 (Nozières-Vinen theory).<sup>11</sup> It is not clear whether the disagreement of our work with previous results can be attributed to electron spin-applied field interaction, to the high  $\kappa_G$  of our alloy, to its extreme "dirtiness" (high  $\xi_0/l$ ), or to some combination of these factors.

We thank D. M. Sellman for able assistance with the measurements; H. Nadler, R. G. Herron, and P. Q. Sauers for careful specimen preparation; C. G. Rhodes and R. A. Spurling for metallography; S. J. Williamson for valuable discussions; and A. S. Joseph for generously allowing our use of his 22-in. Varian magnet facilities.

<sup>28</sup> Using the present techniques we have corroborated this result for annealed Nb-50 at.% Ta. For this alloy the  $J$  dependence of  $\tan\theta$  is less than that shown in Fig. 1.

## Superconductivity in Granular Aluminum Films

ROGER W. COHEN AND B. ABELES

*RCA Laboratories, Princeton, New Jersey*

(Received 13 November 1967)

A detailed description is given of the preparation of granular aluminum films (grain sizes less than 40 Å) with stable superconducting transition temperatures  $T_c$  up to 3.7°K. We present new experimental data of energy gaps, parallel critical fields, and critical current densities. The results are in good agreement with the predictions of the theories of granular superconductors. However, it is found that none of the mechanisms offered so far for the enhancement of  $T_c$  can satisfactorily account for all the properties of the enhanced  $T_c$  granular films.

### I. INTRODUCTION

IT has been known for many years that some superconductors, when composed of small grains (20 to 200 Å), have superconducting transition temperatures  $T_c$  appreciably higher than the ordinary values. Such films were prepared<sup>1-3</sup> by evaporation on to substrates held at 4.2°K. However, upon warming to room temperature, grain growth occurred, and the  $T_c$ 's returned to the usual values. More recently, high  $T_c$  films of the same metals were prepared by evaporation in an

oxygen atmosphere.<sup>4,5</sup> The observed increases in the  $T_c$ 's were of the same magnitude as those obtained by the low-temperature evaporation technique, but they did not change upon storing at room temperature. Furthermore, these films exhibited very high critical magnetic fields and very high normal resistivities.<sup>6</sup> It is believed that these properties resulted from the precipitation of oxygen at the grain boundaries in the form of oxide. The oxide (a) prevented recrystallization and grain growth, thereby stabilizing  $T_c$ , and

<sup>1</sup> A. Shalnikov, *Nature* **142**, 74 (1938); *Zh. Eksperim. i Teor. Fiz.* **10**, 630 (1940).

<sup>2</sup> W. Buckel and R. Hilsch, *Z. Physik* **131**, 420 (1952); **138**, 109 (1954).

<sup>3</sup> N. V. Zavaritzkii, *Dokl. Akad. Nauk SSSR* **82**, 229 (1952).

<sup>4</sup> B. Abeles, R. W. Cohen, and G. W. Cullen, *Phys. Rev. Letters* **17**, 632 (1966).

<sup>5</sup> R. W. Cohen, B. Abeles, and G. S. Weisbarth, *Phys. Rev. Letters* **18**, 336 (1967).

<sup>6</sup> B. Abeles, Roger W. Cohen, and W. Stowell, *Phys. Rev. Letters* **18**, 902 (1967).

TABLE I. Properties of aluminum films evaporated from tungsten filaments.

Sample	$P$ (Torr)	$T_s$ (°K)	$b$ (Å)	$d$ (Å)	$\rho(300)$ ( $\mu\Omega$ cm)	$\rho(4.2)$	$T_c$ (°K)
A	$1 \times 10^{-6}$	300	900	1000	4.2	1.5	$< 1.26^a$
B	$4 \times 10^{-6}$	300	850	400	5.1	2.4	$< 1.26^a$
C	$1 \times 10^{-5}$	300	700	180	14	10	1.60
D	$1.5 \times 10^{-5}$	300	800	90	60	53	2.13
E	$3 \times 10^{-5}$	300	300	60	160	153	2.18
F	$6 \times 10^{-5}$	300	750	45	520	520	2.31
G	$6 \times 10^{-5}$	300	700	$< 40$	1000	1000	2.18
H	$3.5 \times 10^{-5}$	110	...	$< 40$	...	...	2.9

<sup>a</sup> The lowest temperature to which our cryostat could be pumped down was 1.26°K.

(b) formed tunneling barriers between grains resulting in the high normal resistivities, high critical fields, and type-II behavior. We shall refer to a system of superconducting grains separated by tunneling barriers as a "granular superconductor."<sup>7</sup>

The properties of the granular superconductor which we are concerned with in this paper are (a) the enhancement of  $T_c$  and (b) the usual properties of a superconductor (critical field, critical current, energy gap, etc.). Detailed descriptions of the preparation of granular aluminum films are given and new experimental data of energy gaps and parallel critical magnetic fields are presented. Existing theories of granular superconductors are discussed in the light of present experimental evidence.

## II. EXPERIMENTAL

Granular superconducting Al films have been prepared by evaporation in an oxygen atmosphere onto substrates whose temperature was varied between 100 and 300°K. The oxygen provided nucleation centers for the formation of very small particles. The films were 0.1 cm wide and 300–900 Å thick. The substrates were usually glass microscope slides. No discernable difference was observed in the properties of the films when single-crystal quartz, sapphire, or germanium substrates were used.

Two different evaporation techniques were employed. In one, the aluminum was evaporated from a wetted tungsten filament at a rate of about 100 Å/sec. A partial oxygen pressure was maintained during the evaporation by bleeding oxygen into the evaporator and simultaneously pumping on the system with a 4-in.-diam diffusion pump. When the aluminum evaporation started, the oxygen pressure in the system

dropped by about a factor of 2 because of getter action of the aluminum. An alternative, more convenient, technique for producing the high  $T_c$  films was to evaporate aluminum from alumina boat inserts.<sup>8</sup> In this case, no external supply of oxygen was necessary. During the evaporation, the pressure in the system increased from the initial value of  $10^{-6}$  Torr to the value of  $3 \times 10^{-5}$  to  $10^{-4}$  Torr. This increase in pressure was believed to be due to outgassing from the heated alumina boat which provided an internal supply of oxygen. The evaporation rate of the aluminum was 25 Å/sec.

In Table I are listed the properties of films prepared by evaporation from tungsten filaments. Here  $P$  is the oxygen pressure measured during the evaporation,  $T_s$  is the substrate temperature,  $b$  is the sample thickness,  $d$  is the average grain size,  $\rho$  is the normal resistivity, and  $T_c$  is the critical temperature. The thickness of the films was determined by the Tolanski interferometric technique. The grain size was determined by electron microscopy. The distribution of grain sizes in a given film had a standard deviation of about  $d \pm 0.5d$ . Typical micrograms are given in Ref. 4.

Oxygen and substrate temperature affected the properties of the films as follows. With increasing oxygen pressure, the grain size decreased and the normal resistivity increased. At about  $6 \times 10^{-5}$  Torr oxygen, the grain size was less than the resolution limit of the electron microscope (40 Å). For  $T_s = 300^\circ\text{K}$ , films prepared at oxygen pressures in excess of  $6 \times 10^{-5}$  Torr had resistivities in the range 1–100 k $\Omega$  cm at 300°K. The resistivities of these films increased with decreasing temperature, and they remained normal down to the lowest measureable temperature (1.25°K). Less oxygen was required to achieve a given increase in  $T_c$  in a film evaporated on a low-temperature substrate than in a film evaporated onto a higher temperature substrate.

In Table II are listed the transition temperatures

<sup>7</sup> This term was used by R. H. Parmenter [Phys. Rev. **154**, 353 (1967)].

<sup>8</sup> The boats consisted of inserts, conical in shape, pressed out of aluminum, fired and fitted into molybdenum-wire boats.

TABLE II. Properties of aluminum films evaporated from alumina boats.

Sample	$T_s$ (°K)	$T_c$ (°K)
<i>K</i>	300	2.39
<i>L</i>	225	2.35
<i>M</i>	175	2.95
<i>N</i>	157	3.02
<i>O</i>	140	3.28
<i>P</i>	125	3.74

for several films evaporated from alumina boats onto substrates held at various temperatures  $T_s$ . The average grain size in these films was about 40 Å. Since, in this method of evaporation, oxygen pressure was not controlled externally, the normal resistivities had no apparent correlation to  $T_s$  and varied over the range 20–600  $\mu\Omega$  cm. However, the  $T_c$ 's show a monotonic increase as  $T_s$  is lowered from 300 to 125°K. If the substrate was lowered below 125°K, one obtained completely insulating films.

The width of the resistive transitions of the films evaporated by either of the two techniques was usually of the order of 0.01°K. Emission-spectroscopy studies placed an upper limit of 0.1% on metallic impurities in the films.

### III. CRITICAL MAGNETIC FIELDS

It has been shown<sup>6</sup> that transport in a system of clean metallic slabs separated by  $\delta$ -function tunneling barriers of transmission coefficient  $t$  for electrons at normal incidence can be characterized by an effective mean free path  $l_{\text{eff}}$ ,

$$l_{\text{eff}} = dt / (1 - t), \quad (1)$$

where  $d$  is the average spacing between barriers. The normal resistivity  $\rho_n$ , arising from scattering by the barriers, is given by

$$\rho_n^{-1} = \frac{2}{3} N_0 e^2 v_F l_{\text{eff}}, \quad (2)$$

where  $N_0$  is the density of electronic states at the Fermi level, and  $v_F$  is the Fermi velocity. The superconducting state is described by a Landau-Ginzburg equation with a coherence length  $\xi(T)$  near  $T_c$ , given by

$$\xi(T) = 0.85 [\xi_0 l_{\text{eff}} T_c / (T_c - T)]^{1/2}, \quad (3)$$

where  $\xi_0$  is the Pippard coherence length. The bulk critical field  $H_{c2}$  is given by the usual relation:

$$H_{c2} = \Phi_0 / 2\pi \xi^2(T), \quad (4)$$

where  $\Phi_0$  is the flux quantum. Equations (2) and (3) are valid for  $\xi(T) \gg d$ . This inequality guarantees coherence over many grains.

Parmenter<sup>7</sup> has formulated a theory of the granular superconductor, using the isospin formalism to describe

a system of superconducting grains which are weakly coupled ( $t \ll 1$ ) by Josephson tunneling barriers. The author obtained a Landau-Ginzburg-like equation, valid at absolute zero, with an effective coherence length<sup>9</sup>  $\xi(0)$ , given by

$$\xi(0) = \frac{1}{2} \pi (\frac{1}{3} N_0 V)^{1/2} (\xi_0 l_{\text{eff}})^{1/2}. \quad (5)$$

Here  $V$  is the BCS effective electron-phonon interaction. Apart from a numerical factor of order unity, Eq. (5) is identical to the temperature-independent part of Eq. (3).

The experimental quantities that we wish to compare with theory are the parallel  $H_{\parallel}$  and perpendicular  $H_{\perp}$  critical magnetic fields. Since our films are dirty type-II superconductors, the perpendicular critical field  $H_{\perp}$  is given by the bulk critical field  $H_{c2}$ . For a type-II superconductor, the ratio  $H_{\parallel}(T)/H_{\perp}(T)$  is a function of the dimensionless quantity<sup>10,11</sup>  $b/\xi(T)$ . This result is also expected to hold for a granular superconductor, provided  $\xi(T) \gg d$ . The limiting values of the ratio  $H_{\parallel}/H_{\perp}$  are  $H_{\parallel}/H_{\perp} = 1.69$  for the case  $b/\xi(T) \gg 1$  and  $H_{\parallel}/H_{\perp} = (12)^{1/2} [\xi(T)/b]$  for the case  $b/\xi(T) \ll 1$ .

Parallel and perpendicular critical fields were determined by measuring the dc resistance as a function of magnetic field at constant measuring currents. A four-probe technique was employed. The current level was sufficiently low so that the resistive transitions were independent of current. The critical field was defined as that field for which the resistance attained

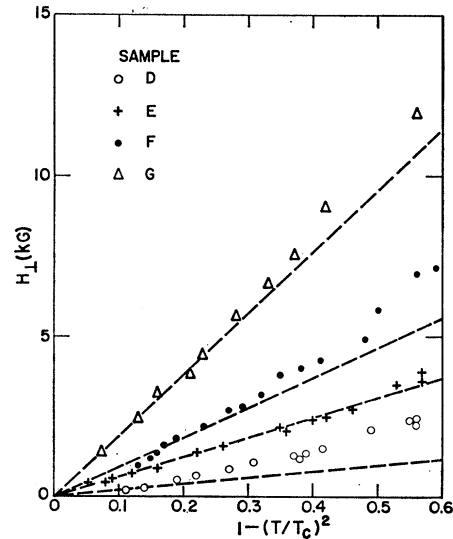


Fig. 1. Critical field  $H_{\perp}$  as a function of  $[1 - (T/T_c)^2]$  for four of the samples listed in Table I.

<sup>9</sup> R. H. Parmenter, Phys. Rev. **158**, 314 (1967).

<sup>10</sup> J. P. Burger, A. Deutscher, E. Guyon, and A. Martinet, Phys. Rev. **137**, A853 (1965).

<sup>11</sup> D. Saint-James and P. G. de Gennes, Phys. Letters **5**, 306 (1963).

TABLE III. Some characteristic parameters of granular aluminum films.

Sample	$l_{\text{eff}}^{(\rho)}$ (Å)	$l_{\text{eff}}^{(H)^a}$ (Å)	$(\xi_0 l_{\text{eff}}^{(H)})^{1/2}$ (Å)	$\lambda_L (\xi_0 / l_{\text{eff}}^{(H)})^{1/2}$ (Å)	$t$
D	27	14	350	3900	0.13
E	10	5	210	6600	0.08
F	3	3	160	8400	0.06
G	1.6	1.4	110	12000	0.03

<sup>a</sup> In calculating the values of  $l_{\text{eff}}^{(H)}$  from experimental data, the Pippard coherence length  $\xi_0 = \hbar v_F / \pi \Delta(0)$  used was obtained by multiplying the

value  $\xi_0 = 16\,000$  Å for ordinary Al by the ratio of the energy gap  $\Delta$  of ordinary Al to that of the enhanced  $T_c$  film.

one-half its normal-state value. The widths of the transitions were about 30% of the critical field.

The perpendicular critical field  $H_{\perp}$  on four of the samples given in Table I have already been published,<sup>6</sup> and we reproduce them in Fig. 1. In Table III are listed the values of the effective mean free path  $l_{\text{eff}}^{(\rho)}$  for these four samples, calculated from Eq. (2) using the measured resistivity at 4.2°K and the value<sup>12</sup>  $\rho_n l_{\text{eff}}^{(\rho)} = 1.6 \times 10^{-11} \Omega \text{ cm}^2$ . The values of  $l_{\text{eff}}^{(H)}$ , given in Table III, were calculated from Eqs. (3) and (4), using the measured values of  $dH_{\perp}/dT|_{T_c}$ . As can be seen from the table, the mean free paths obtained by the two methods are in good agreement with each other. We have also included in the table the values of the temperature-independent part of the coherence length  $(\xi_0 l_{\text{eff}}^{(H)})^{1/2}$  and the penetration depth  $\lambda_L [\xi_0 / l_{\text{eff}}^{(H)}]^{1/2}$  ( $\lambda_L = 157$  Å is the London penetration depth at  $T=0$ ). In the last column of Table III are given the barrier-transmission coefficients  $t$ , calculated from Eq. (1), using the values of  $l_{\text{eff}}^{(H)}$  and the values of  $d$  given in Table I. We see from the table that indeed  $\xi(T) \gg d$ , so that the use of Eqs. (3) and (4) is justified. Furthermore, we call attention to the unusually large values of the penetration depth. Also, we note that the values of  $t$  are many orders of magnitude larger than those

for ordinary tunnel junctions, indicating that the grains are strongly coupled to each other.

In Fig. 2 are presented the parallel-critical-field  $H_{\parallel}$  data, obtained on the same four samples. In Fig. 3, we have plotted the anisotropy ratio  $H_{\parallel}(T)/H_{\perp}(T)$  for these samples as a function of the reduced quantity  $[b/2\xi(T)]^2$ . The dashed curve in Fig. 3 represents the theoretical dependence<sup>10,11</sup> of  $H_{\parallel}/H_{\perp}$  on  $[b/2\xi(T)]^2$ . We note that although the measured anisotropy is consistently larger than the theoretical prediction, there is qualitative agreement with theory in that (a) in the region  $b/\xi(T) > 1$  ( $H_{c3}$  regime), the experimental  $H_{\parallel}/H_{\perp}$  approaches the constant value 2.0, which is close to the theoretical value 1.69, and (b) in the region  $b/\xi(T) \lesssim 1$  (thin-film regime),  $H_{\parallel}/H_{\perp}$  increases rapidly. This behavior leads us to conclude that the effect of the granular structure is entirely included in the coherence length  $\xi$ , so that the appropriate quantity determining the anisotropy ratio of a film with a given  $\xi$  is the film thickness.

#### IV. CRITICAL CURRENT

The expression for the critical current density  $J_c$  at  $T=0^\circ\text{K}$  of a granular superconducting film whose thickness is small compared to  $\xi(0)$  was derived by

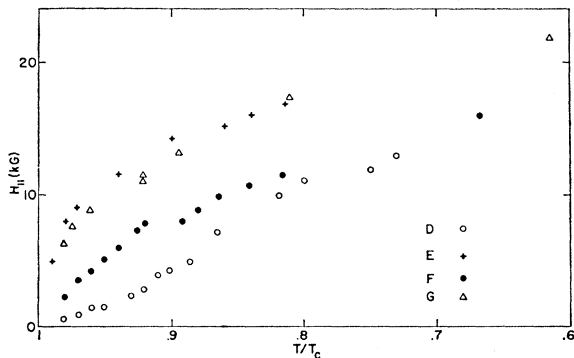


FIG. 2. Critical field  $H_{\parallel}$  as a function of  $T/T_c$  for four of the samples listed in Table I.

<sup>12</sup> J. L. Olsen, *Electron Transport in Metals* (Interscience Publishers, Inc., New York, 1962), p. 84.

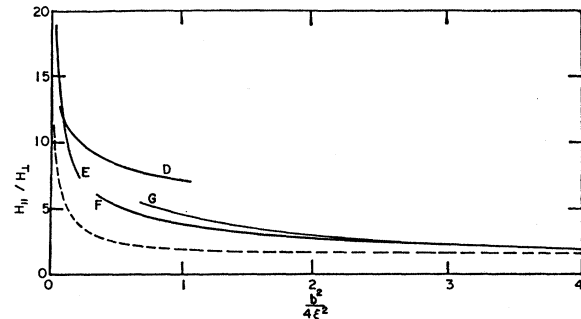


FIG. 3. Anisotropy ratio  $H_{\parallel}/H_{\perp}$  versus the reduced quantity  $b^2/4\xi^2$ . The full curves are the ratios of the smoothed values of  $H_{\parallel}$  to  $H_{\perp}$  obtained from Figs. 1 and 2. The dashed curve was obtained from the theoretical relationship of Saint-James and de Gennes (Ref. 11).

TABLE IV. Critical currents in granular aluminum films.

Sample	$\rho(4.2^\circ)$ ( $\mu\Omega$ cm)	$I_c$ (mA)	$w/\lambda$	$b/\lambda$	$J(\text{center})$ ( $10^6\text{A}/\text{cm}^2$ )	$J(\text{edge})$	$J_c$
K	90	32	$2 \times 10^4$	0.14	0.04	1.3	1.4
F	520	11	$1 \times 10^4$	0.09	0.016	0.29	0.6

Parmenter<sup>7</sup> and is given by

$$J_c = (4e\xi(0)/\hbar V)\Delta^2(0), \quad (6)$$

where  $\Delta(0)$  is the superconducting energy gap at  $T=0^\circ\text{K}$ .

The critical currents  $I_c$  measured at  $1.3^\circ\text{K}$  and the normal resistivities of the granular films are given in Table IV. The critical currents were determined by the onset of a detectable resistance in the Al films, approximately  $10^{-5}$  of the normal resistance of the films. In order to compare the experimental critical current with the theoretical prediction, it is necessary to know the current distribution within the film. This distribution is determined by the parameters  $w/\lambda$  and  $b/\lambda$ , where  $w$ ,  $b$ , and  $\lambda$  are, respectively, the width, the thickness, and the penetration depth of the films. The values of these ratios for our films are given in Table IV.

Marcus<sup>13</sup> derived from the London equation numerical solutions for the current-density distribution  $J$ . He finds that in the ranges  $10 \leq w/\lambda \leq 500$  and  $1 \leq b/\lambda \leq 5$ ,  $J$  peaks at the edges and is nearly uniform in the region several penetration lengths away from the edges. He estimates the following for the ratio of the current at the center to that at the edge<sup>14</sup>:

$$J(\text{center})/J(\text{edge}) = 1.65\lambda/(wb)^{1/2}. \quad (7)$$

Since in our case  $w/\lambda$  is very large, we shall assume that  $J(\text{center})$  is given by the average current density  $I_c/wb$ . Furthermore, since for our films  $\lambda(wb)^{-1/2} \ll 1$ , Eq. (7) is expected to be a reasonable approximation, and we shall use it to calculate  $J(\text{edge})$ . The values of  $J(\text{center})$  and  $J(\text{edge})$  determined in this manner are given in Table IV and are compared with the theoretical current densities  $J_c$ . The values of  $J_c$  were calculated from Eq. (6), using Eq. (5) for  $\xi(0)$ . The interaction  $V$  was computed from the BCS equation for  $T_c$

$$kT_c = 1.13 \langle \hbar\omega \rangle \exp(-1/N_0V),$$

with<sup>15</sup>  $\langle \hbar\omega \rangle = \frac{1}{2}\theta_D = 210^\circ\text{K}$ ,  $N_0 = 2.2 \times 10^{34} \text{ erg}^{-1} \text{ cm}^{-3}$  (determined from specific-heat measurements on ordinary<sup>16</sup> Al), and the measured  $T_c$ 's. The effective mean free paths  $l_{\text{eff}}$  were determined from the normal resistivities, using Eq. (2). The gaps  $\Delta(0)$  were deter-

mined from the  $T_c$ 's, using the experimental relation  $2\Delta(0)/kT_c = 3.45$ . The agreement between the values of  $J(\text{edge})$  and  $J_c$  is good, in spite of the crudeness of the above approximations and the fact that Eq. (6) for  $J_c$  applies only for a film  $b < \xi(0)$ , which was not the case for our films.

## V. ENERGY GAP

The energy gaps of the granular films were determined from tunneling measurements on Al-Al<sub>x</sub>O<sub>y</sub>-Pb and Al-Al<sub>x</sub>O<sub>y</sub>-Sn junctions. The junctions were prepared in the usual crossed-strip configuration by first evaporating the Al film in the form of a 1-mm-wide and about 1000 Å thick strip, allowing it to oxidize in oxygen for about 2 min, and then evaporating the Pb or Sn film on top of the Al. In Fig. 4 is shown the conductance  $dI/dV$  vs voltage  $V$  characteristics of an Al-Al<sub>x</sub>O<sub>y</sub>-Sn junction taken at  $1.3^\circ\text{K}$ . The criteria for establishing the value of the Sn gap  $\Delta_{\text{Sn}}$  and the Al gap  $\Delta_{\text{Al}}$  are: (a) The value of  $(\Delta_{\text{Sn}} - \Delta_{\text{Al}})$  is given by the position of the conductance maximum due to thermally excited quasiparticles; and (b) the point  $(\Delta_{\text{Sn}} + \Delta_{\text{Al}})$  is established according to the criterion of Douglass and Meservey,<sup>17</sup> i.e.,

$$dI/dV |_{V=(\Delta_{\text{Sn}}+\Delta_{\text{Al}})} = dI/dV |_{V=(\Delta_{\text{Sn}}-\Delta_{\text{Al}})}.$$

The  $T_c$ 's defined by the vanishing of  $\Delta$  agreed with the  $T_c$ 's determined by the resistive transitions.

In Fig. 5 is shown the temperature dependence of the superconducting energy gap  $\Delta(T)$  for three of the Al films given in Table II. The solid curves represent

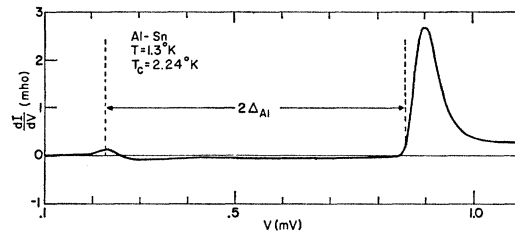


FIG. 4. Conductance  $dI/dV$  versus voltage  $V$  characteristic of an Al-Al<sub>x</sub>O<sub>y</sub>-Sn junction measured at  $1.3^\circ\text{K}$ . The energy gap of aluminum  $2\Delta_{\text{Al}}$  is indicated in the figure.

<sup>15</sup> D. Pines, Phys. Rev. **109**, 280 (1958).

<sup>16</sup> *Handbook of Chemistry and Physics*, edited by C. D. Hodgman (Chemical Rubber Publishing Co., Cleveland, Ohio, 1965), 46th ed., p. E67.

<sup>17</sup> D. H. Douglass, Jr., and R. Meservey, Phys. Rev. **135**, A19 (1964).

<sup>13</sup> P. M. Marcus, in *Proceedings of the Seventh International Conference on Low-Temperature Physics, 1960*, edited by G. M. Graham and A. C. Hollis (University of Toronto Press, Toronto, Canada, 1960), p. 418.

<sup>14</sup> P. M. Marcus (private communication).

the BCS temperature dependence<sup>18</sup> for  $\Delta(T)$  for the indicated values of  $T_c$  and  $2\Delta(0)/kT_c=3.45$ . The fit of the experimental data to the theoretical curves is very good for all three films.

No detectable broadening of the aluminum energy gaps, in addition to the usual thermal broadening, was observed. This result is surprising, for one might have expected a distribution in energy gaps resulting from the inhomogeneous granular structure of the films. As we shall see, the lack of broadening has important consequences in the interpretation of the enhancement of  $T_c$ .

## VI. MECHANISMS OF ENHANCEMENT OF $T_c$

Several mechanisms have been proposed to explain the enhanced  $T_c$ 's. We shall now discuss these mechanisms in the light of available experimental evidence.

### A. Quantization of Electronic Motion

Thomson and Blatt<sup>19</sup> have shown that quantization of electronic motion in very thin films can result in an increased transition temperature. It has been pointed out that such an effect can also result in the enhancement of the  $T_c$  of a system of small isolated grains.<sup>4</sup> The calculated enhancement was of the same magnitude as that observed experimentally. Parmenter has also calculated the enhancement of  $T_c$  due to quantization of motion.<sup>20</sup> The author found that the enhancement could be described by an increased effective electron-phonon interaction  $V$ . He obtained the result that  $T_c$  is double the ordinary value when the grain size is equal to the characteristic length  $L=(\lambda_F^2\xi_0)^{1/3}$ , where  $\lambda_F$  is the Fermi wavelength. For aluminum,  $L=62$  Å. Furthermore, Parmenter found that the gap  $\Delta(0)$  increases somewhat faster than  $T_c$ , so that the quantity  $2\Delta(0)/kT_c$  increases from the BCS value of 3.528 to the value 4 in the case  $d\ll L$ .

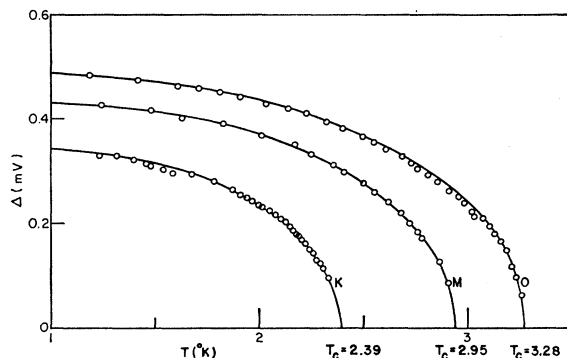


FIG. 5. The energy gap  $\Delta$  as a function of temperature for three of the aluminum films listed in Table II. The values of  $T_c$  are indicated in the figure, and the substrate temperatures  $T_s$  are given in Table II. The solid lines represent the BCS temperature-dependent gap function  $\Delta(T)$ , with  $2\Delta(0)/kT_c=3.45$ .

<sup>18</sup> J. Bardeen, L. N. Cooper, and J. R. Schrieffer, Phys. Rev. **108**, 1175 (1957).

<sup>19</sup> J. Thomson and J. M. Blatt, Phys. Letters **5**, 6 (1963).

<sup>20</sup> R. H. Parmenter, Phys. Rev. **167**, 387 (1968).

Experimentally, we find that in aluminum films  $T_c$  is double the ordinary value when the average grain size is 80 Å. This is of the same magnitude as the theoretical value  $L=62$  Å. Furthermore, with enhanced  $T_c$ 's in the range  $2.4 < T_c < 3.3^\circ\text{K}$ , we have determined the ratio  $2\Delta(0)/kT_c=3.45$ . This is to be compared with the value for ordinary<sup>17</sup> Al ( $T_c=1.18^\circ\text{K}$ ),  $2\Delta(0)/kT_c\approx 3.3$ . This increase of  $2\Delta(0)/kT_c$  with  $T_c$  is consistent with the theory. However, it should be pointed out that this is by no means the only mechanism which can account for the increase in  $2\Delta(0)/kT_c$ . For instance, the effect could be due to a rise in  $2\Delta(0)/kT_c$  as gap anisotropy is washed out by impurity scattering.<sup>21</sup>

Although the above mechanism is able to account qualitatively for the observed enhancement, we do not believe that the idealized model of isolated grains of equal size applies to the granular films prepared by low-temperature deposition or by the technique described here. In these films, there is a wide distribution of grain sizes, and the grains are not completely isolated. As we shall discuss below, these two factors have important consequences which are not accounted for by the theory.

Because of incomplete isolation of individual grains, the discrete energy levels of the isolated grains broaden into bands. The model of quantization of electronic motion breaks down when the width of the bands near the Fermi level becomes of the order of the spacing between bands. Solving the one-dimensional Schrödinger equation for an array of  $\delta$ -function barriers separated by a distance  $d$  (Kronig-Penney model), we estimate that the above condition is met for  $t\gtrsim 0.5$ . The lowest resistivities observed in films with  $T_c\sim 3^\circ\text{K}$  and  $d\sim 40$  Å was about  $20\ \mu\Omega\ \text{cm}$ , corresponding to  $t\sim 0.7$ , indicating that, for such samples, the broadening of the one-electron energy levels may be severe. Thus the model is probably not applicable to these low-resistivity films.

Another serious objection concerns the effect of the distribution of grain sizes in our films. This distribution is expected to result in a corresponding distribution in energy gaps, and this should lead to a broad tunneling density of states. This is contrary to experimental observation, where the observed  $dI/dV$  characteristics exhibit extremely sharp energy gaps. To estimate the smearing predicted by the theory, we consider two superconducting grains in the shape of cubes with edges  $d_1$  and  $d_2$  [ $d_1, d_2\ll\xi(T)$ ], which are separated by a tunneling barrier of transmission coefficient  $t$ . In the case  $t=1$ , the usual condition of continuity of the quantity  $\Delta/N_0V$  applies,<sup>22</sup> and consequently

$$\Delta_2/\Delta_1 = V_2/V_1, \quad (8)$$

where  $V_1$  and  $V_2$  are the effective electron-phonon interactions in cubes 1 and 2, respectively. Taking

<sup>21</sup> J. R. Clem, Ann. Phys. (N.Y.) **40**, 268 (1966).

<sup>22</sup> P. G. de Gennes, Rev. Mod. Phys. **36**, 225 (1964).

the average grain size equal to  $L$ , and representing the observed spread of grain sizes by  $d_1=1.5L$  and  $d_2=0.5L$ , we estimate from Parmenter,<sup>20</sup>  $(V_2-V_1)/V_1=(\Delta_2-\Delta_1)/\Delta_1\sim 0.3$ . In this calculation, we have used the value  $N_0V=0.19$  for bulk Al. The above estimated value of the spread of energy gaps is a lower limit, because as  $t$  decreases from unity, the interaction between grains decreases, and the difference between the gaps becomes much larger. In the limit of isolated grains ( $t\rightarrow 0$ ),  $\Delta_2/\Delta_1\approx \exp[(1/N_0V_1)-(1/N_0V_2)]\sim 3$ .

### B. Surface Enhancement

Ginzburg<sup>23</sup> has suggested that the effective electron-phonon interaction  $V_s$  near the surface of a superconductor-dielectric interface may be larger than that of the bulk  $V_b$ . As examples of possible mechanisms for the increased interaction, the author mentions "exchange of surface phonons and variation of screening." It has also been proposed by Cohen *et al.*<sup>24</sup> that electrons can be paired across an insulating barrier and that the effective attractive interaction for such pairing can be larger than that for pairing between electrons on the same side of the barrier.

The idea of surface enhancement can be applied to granular superconductors if one regards the grain boundaries as internal surfaces.<sup>4,25</sup> In that case, the transition temperature of a granular superconductor [ $\xi(T)\gg d$ ] is given by<sup>4</sup>

$$kT_c=1.13\langle\hbar\omega\rangle\exp(-1/N_0V), \quad (9)$$

$$V=V_b+(V_s-V_b)[1-(1-2d_s/d)^3], \quad \text{for } d_s<\frac{1}{2}d \quad (10a)$$

$$V=V_s, \quad \text{for } d_s\geq\frac{1}{2}d, \quad (10b)$$

where  $\langle\hbar\omega\rangle$  is the BCS cutoff energy and  $d_s$  is the width of the enhanced surface region at the grain boundary. Case (10a) results from proximity effects between the enhanced surface and the ordinary bulk regions,<sup>4</sup> and  $V$  increases with decreasing grain size  $d$ . Case (10b) corresponds to the extreme situation where the enhanced regions encompass the entire superconductor, and  $V$  is independent of grain size.

In order to fit Eq. (9) to the experimental variation of  $T_c$  with grain size, it is necessary for  $2d_s$  to be substantially less than the grain size, so that the case (10a) applies for our films. However, in that case, one would expect two values of the energy gap: a gap  $\Delta_s$  which represents the pairing energy in the surface regions and a gap  $\Delta_b$  which represents the pairing energy in the bulk. The relation between the two gaps is given by Eq. (8). In a previous publication,<sup>4</sup> it was shown that the value  $V_s/V_b=1.42$  accounts for the observed

variation of  $T_c$  with grain size. Thus the multiple gaps may be expected to give rise to a smearing of the effective tunneling density of states over energies of the order of 40% of the gap energy. No such effect has been observed in any of the tunneling curves, which yield very sharp energy gaps for the aluminum (see Fig. 4).

In order to account for the observed sharp energy gaps, it is necessary for the electron-phonon interaction to be constant throughout the material (the case  $d_s>\frac{1}{2}d$ ). The mechanism of Cohen *et al.*,<sup>24</sup> namely, pairing across barriers, would provide for a homogeneous  $V$  because, according to the authors,  $d_s$  can be as large as  $v_F/\langle\omega\rangle\sim$ several hundred angstroms. However, when  $d_s\gtrsim d$ , the transition temperature is independent of grain size, contrary to experimental observation.

The question also arises as to what part is played by the oxide boundaries in determining the magnitude of  $V_s$ . In view of the comparable grain sizes and enhancements of  $T_c$  found in films evaporated at low temperatures without oxygen,<sup>2</sup> it appears that oxide plays no essential role in the surface-enhancement mechanism. However, the oxygen is of course necessary to stabilize the small-grain-size structure.

Surface enhancement can also result from an increase in  $N_0$  near the grain boundaries. Again, as was the case with  $V_s$ , this mechanism would not be compatible with the observed sharp energy gap of the granular aluminum.

### C. Conclusion

We conclude that none of the above mechanisms satisfactorily explains all the properties of the enhanced granular films. In particular, none of the mechanisms can simultaneously account for the observed sharp energy gaps and the variation of  $T_c$  with grain size. It would appear that a requirement of any satisfactory theory of the enhancement is that the dimensionless coupling constant  $N_0V$  be constant throughout the material, yet a function of average grain size. Furthermore, it would have to account for the variation of the enhancement from material to material, and the decrease in  $T_c$  observed in the strong-coupling superconductors<sup>2,26</sup> Hg and Pb.

### ACKNOWLEDGMENTS

We thank J. I. Gittleman for a helpful discussion on critical currents and we thank Dr. P. M. Marcus for making available to us his unpublished work on current distribution in superconducting films. We thank W. Stowell for the measurements of the critical fields and G. Weisbarth for technical assistance. Finally, we wish to thank R. H. Parmenter for stimulating discussions and for making his work available to us prior to publication.

<sup>26</sup> E. T. S. Appleyard, I. R. Bristow, H. London, and A. D. Misner, Proc. Roy. Soc. (London) **A172**, 540 (1939).

<sup>23</sup> V. L. Ginzburg, Phys. Letters **13**, 101 (1964).

<sup>24</sup> M. H. Cohen and D. H. Douglass, Jr., Phys. Rev. Letters **19**, 118 (1967).

<sup>25</sup> O. F. Kammerer and M. Strongin, Phys. Letters **17**, 224 (1965).